Electronic Supplementary Material (ESI) for Journal of Materials Chemistry A.

Supporting information

Defective metal-organic framework derivative by room-temperature exfoliation and reduction for highly efficient oxygen evolution reaction

Zehua Zou, Minmin Cai, Xiaohua Zhao, Junfeng Huang, Jing Du, Cailing Xu*

State Key Laboratory of Applied Organic Chemistry, Laboratory of Special Function Materials and Structure Design of the Ministry of Education, College of Chemistry and Chemical Engineering, Lanzhou University, Lanzhou 730000, China

*Corresponding author: xucl@lzu.edu.cn;

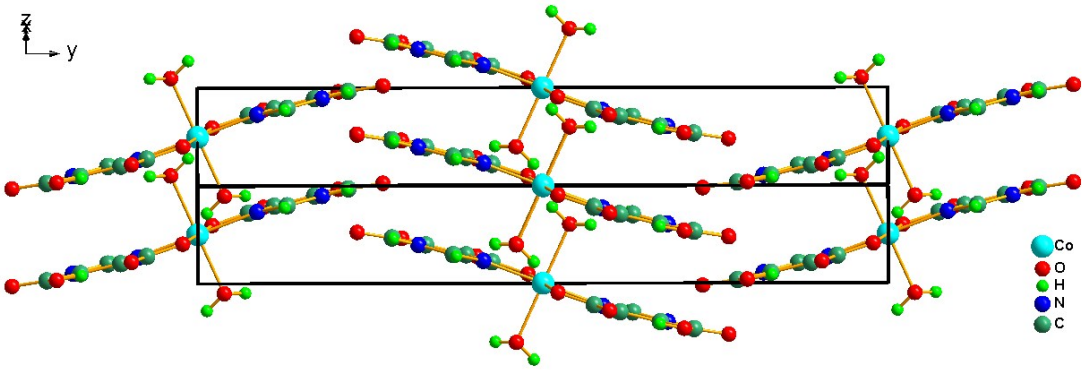

Fig. S1. The crystal structure and coordination of Co-MOF from the Cambridge Crystallographic Data Centre..

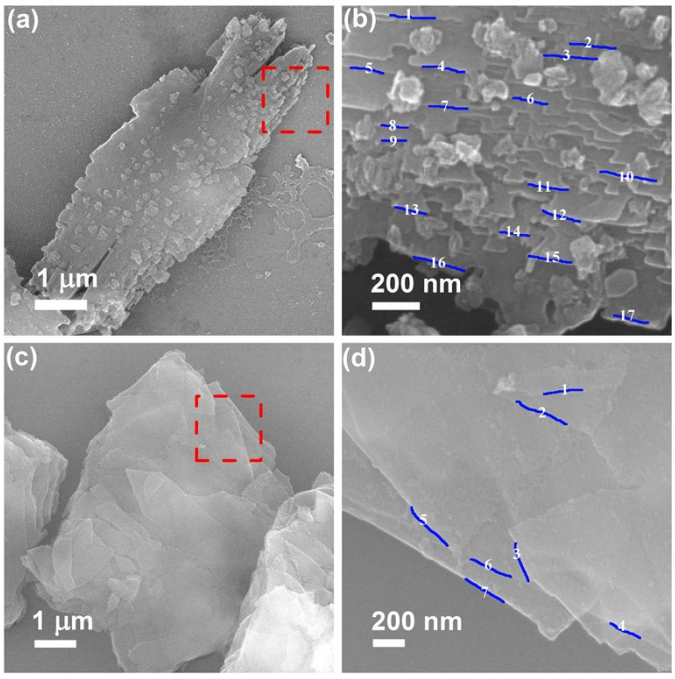

Fig. S2. The multi-layered structure of the Co-MOF (a-b) and CoFe-MOF (c-d).

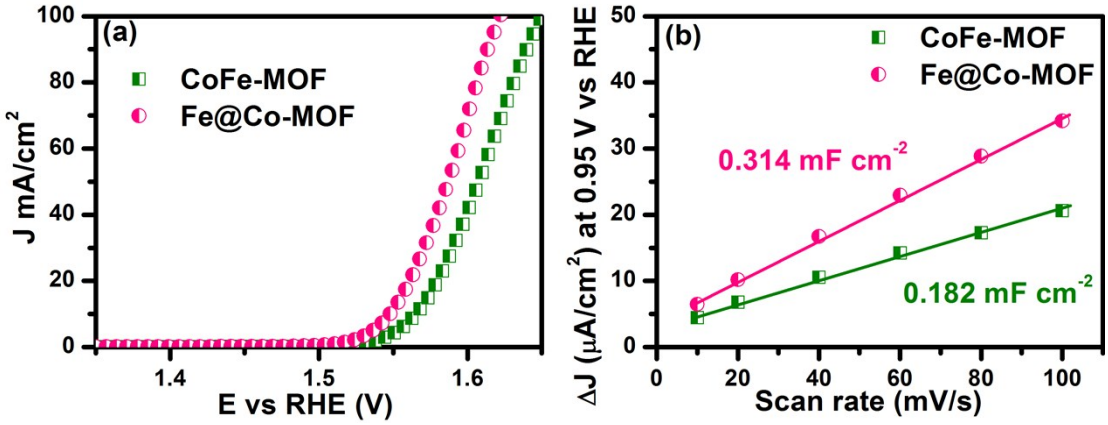

Fig. S3. (a) LSV curves and (b) double-layer capacitance of CoFe-MOF and Fe@Co-MOF.

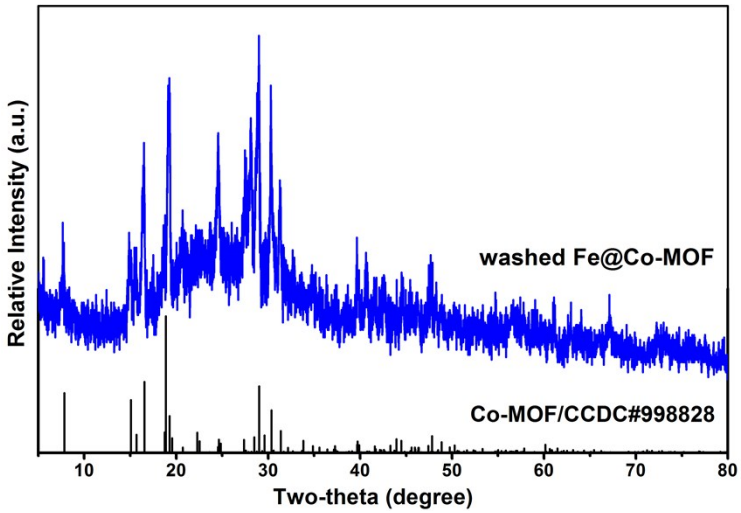

Fig. S4. XRD pattern of Fe@Co-MOF washed by DI-water and the standard card.

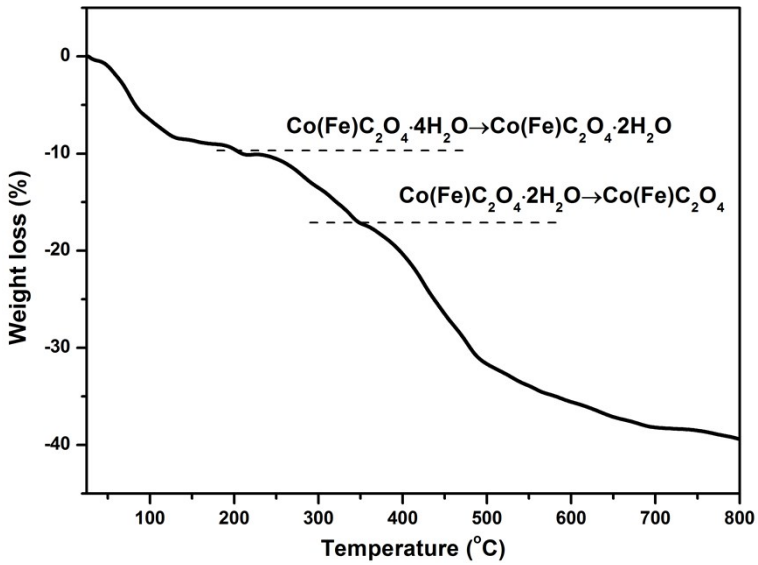

Fig. S5. The TG curve of r-CoFe.

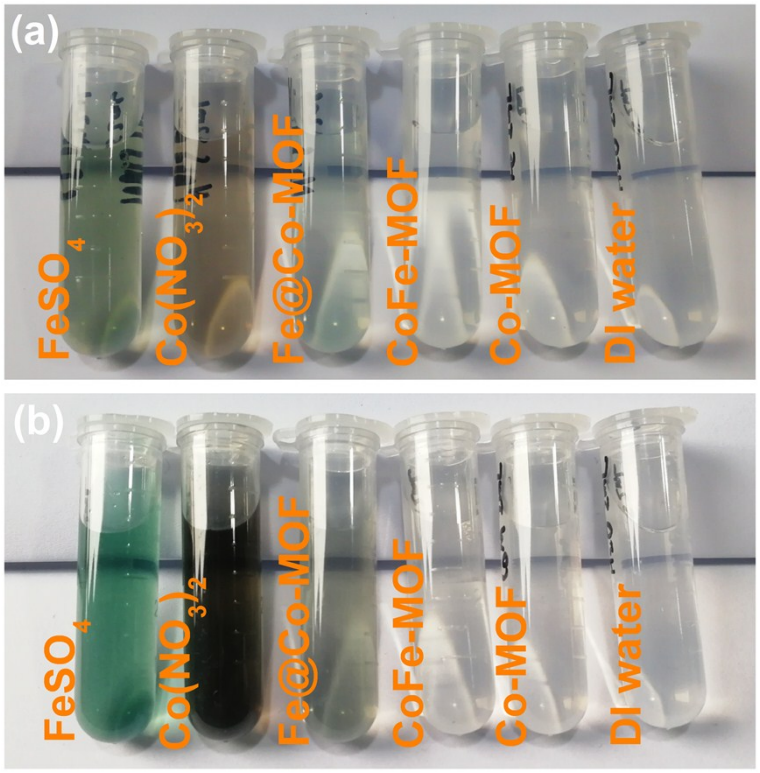

Fig. S6. The photos of dialysate from mother liquid [$FeSO_4$ solution, $Co(NO_3)_2$ solution, Fe@Co-MOF suspension, CoFe-MOF suspension, Co-MOF suspension and DI water, left to right] with the addition of 1 M Na_2S solution after a dialysis for 10 min (a) and 5 h (b). (molecular weight cutoff is 8000-14000)

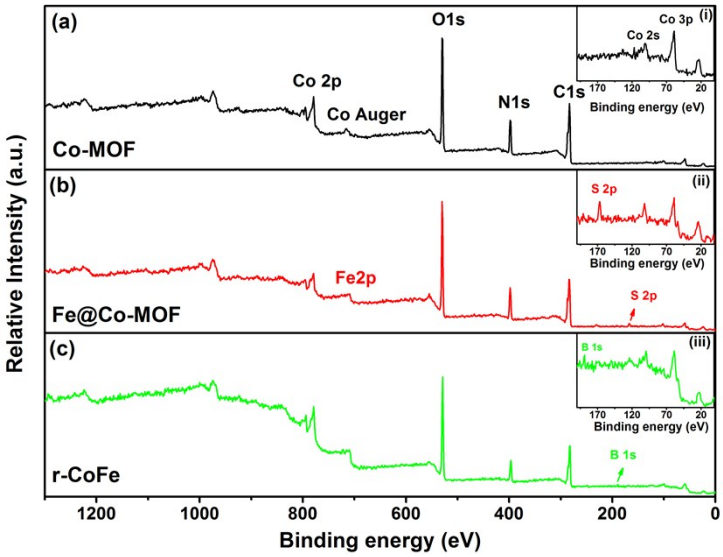

Fig. S7. XPS spectra of Co-MOF (a), Fe@Co-MOF (b) and r-CoFe (c), respectively. Inset: the corresponding magnification (i-iii).

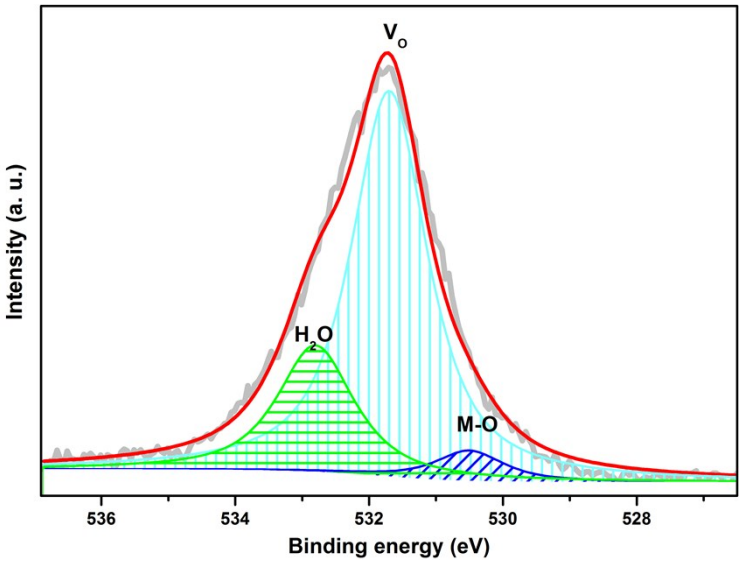

Fig. S8. The XPS fitting of O 1s of r-CoFe.

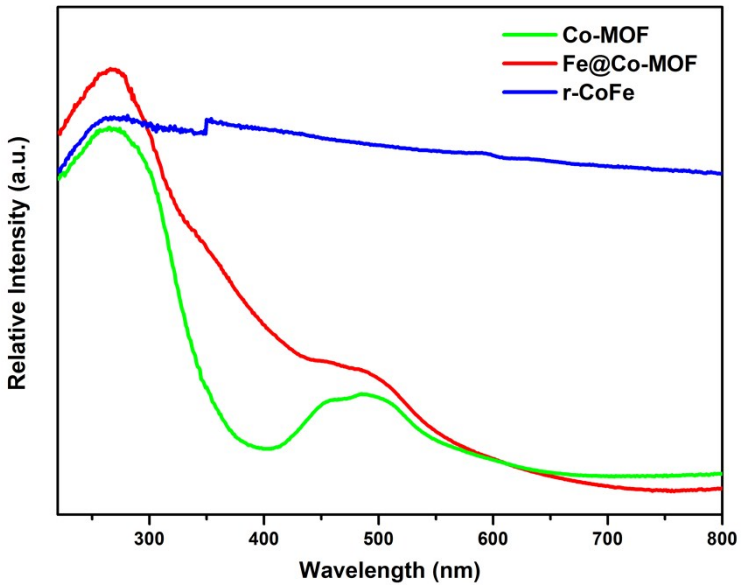

Fig. S9. The UV-vis absorption spectra of Co-MOF, Fe@Co-MOF and r-CoFe.

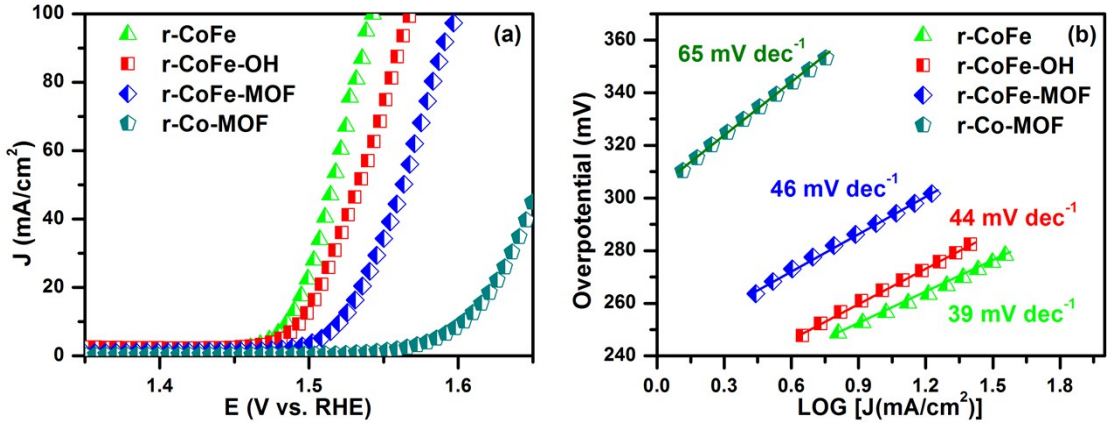

Fig. S10. (a) LSV curves and (b) Tafel plots of r-CoFe, r-CoFe-OH, r-CoFe-MOF and r-Co-MOF, respectively.

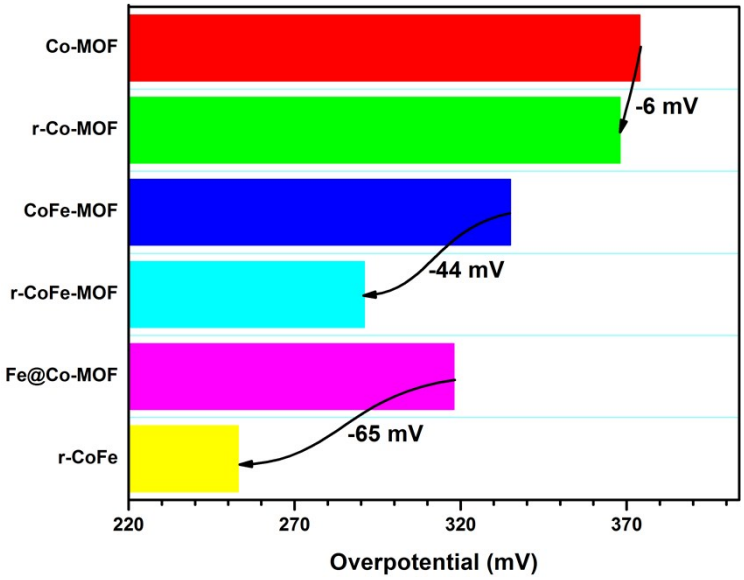

Fig. S11. The summarized overpotentials of Co-MOF, r-Co-MOF, CoFe-MOF, r-CoFe-MOF, Fe@Co-MOF and r-CoFe, respectively.

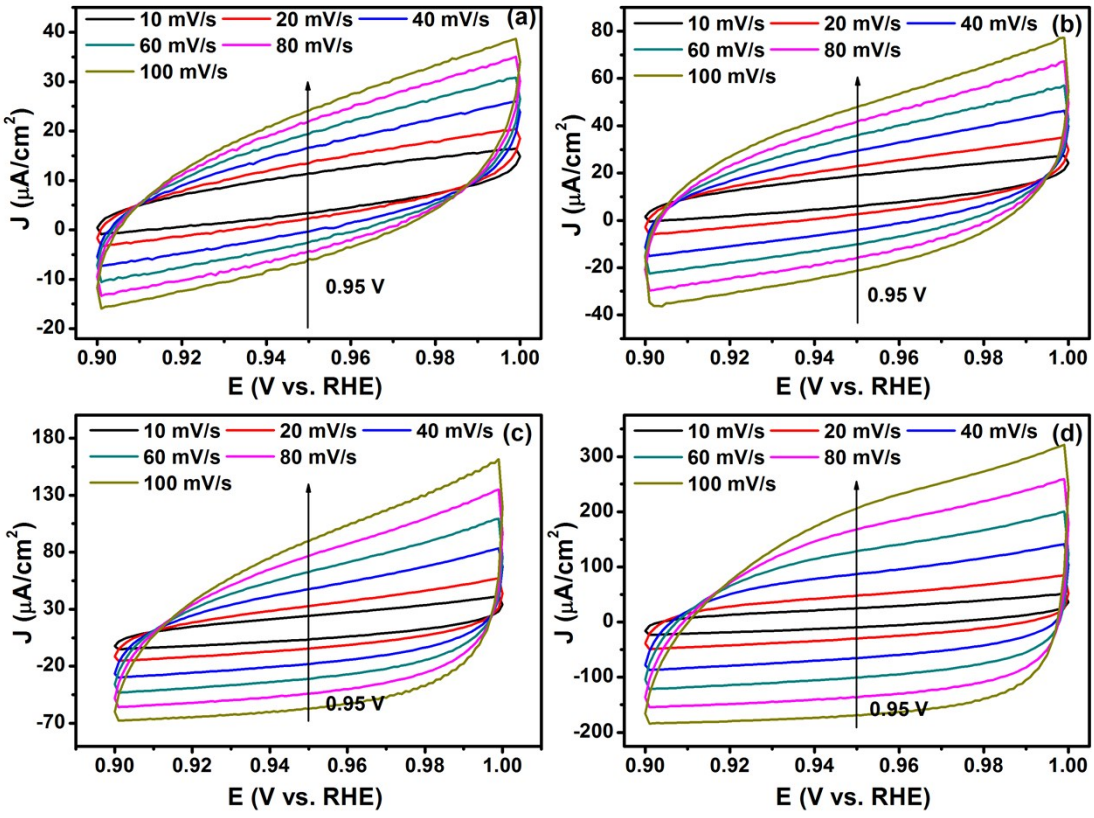

Fig. S12. The CVs measured in a non-Faradaic region of Co-MOF (a), Fe@Co-MOF (b), r-CoFe-OH (c) and r-CoFe (d).

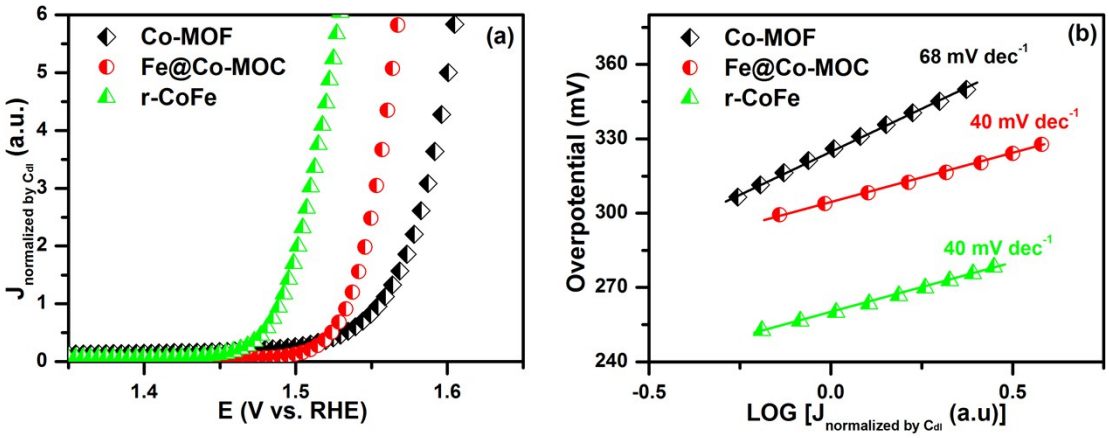

Fig. S13. (a) LSV curves and (b) Tafel plots of Co-MOF,CoFe-MOF and r-CoFe normalized by C_{dl}.

Table S1. The location of XPS fitting peaks and the ratio of peak area.

	*Position Co^{2+} (eV)	**Position Co^{3+} (eV)	***R(Co^{2+}/Co^{3+})
Co-MOF	782.57	781.13	1.22
Fe@Co-MOF	782.76	781.29	1.36
r-CoFe	782.47	781.07	2.03

*: the position of Co^{2+} XPS peak. **: the position of Co^{3+} XPS peak. ***: the ratio of XPS peak area for Co^{2+} and Co^{3+}.

Table S2. Comparisons of OER activities of some representative Co/Fe-based MOF derivatives.

Electrocatalysts	$\eta_{10\ mA\ cm^{-2}}$ (mV)	Tafel slope (mV dec^{-1})	References
r-CoFe	253	39	**This work**
$Co_{0.6}Fe_{0.4}P$-1.125	298	48	*Chem. Sci.*, 2019, **10**, 464-474.
CoFe-MOF-74-400^{o}C-1h	300	-	*J. Am. Chem. Soc.* 2018, **140**, 15336-15341.
FeCo-Co_4N/N-C	280	40	*Adv. Mater.* 2017, **29**, 1704991.
$Co_{0.7}Fe_{0.3}P$/C	270	27	*Nanoscale*, 2018, **10**, 19774-19780.
Co-PBA-plasma-2h	274	53	*Adv. Energy Mater.* 2018, **8**, 1800085.
Co-Fe-P-1.7	244	55	*ACS Appl. Mater. Inter.* 2017, **9**, 362-370.
NF@NC-$CoFe_2O_4$/C	240	45	*Adv. Mater.* 2017, **29**, 1604437.
Fe_1Co_3/Vo-800	250	53	*J. Mater. Chem. A*, 2019, **7**, 3090-3100.
S-$Co_{9-x}Fe_xS_8$@rGO-10	290	66	*Small*, 2018, **14**, 1703748.

Table S3. The ICP results of Co-MOF, Fe@Co-MOF, r-CoFe-OH and r-CoFe (unit: w%).

	Co-MOF	Fe@Co-MOF	r-CoFe-OH	r-CoFe
Co	15.3	11.9	40.0	30.8
Fe	--	5.7	18.2	20.4
B	--	--	6.1	3.0